The Effect of Process Parameters on the Synthesis of Ti and TiO_2 Nanoparticles Producted by Electromagnetic Levitational Gas Condensation

M. Moazeni, M. Moradi, S. Torkan, A. Kermanpur, F. Karimzadeh

Abstract

The nanoparticles of Ti and TiO_2 have attracted extensive research interest because of their diverse applications in, for instance, catalysis, energy conversion, pigment and cosmetic manufacturing and biomedical engineering. Through this project, a one-step bulk synthesis method of electromagnetic levitational gas condensation (ELGC) was utilized for the synthesis of monodispersed and crystalline Ti and TiO_2 nanoparticles. Within the process, the Ti vapours ascending from the high temperature levitated droplet were condensed by an argon gas stream under atmospheric pressure. The TiO_2 nanoparticles were produced by simultaneous injection of argon and oxygen into the reactor. The effects of flow rate of the condensing and oxidizing gases on the size and the size distribution of the nanoparticles were investigated. The particles were characterized by scanning electron microscopy (SEM), X-ray diffraction (XRD) and image analysis. The process parameters for the synthesis of the crystalline Ti and TiO_2 nanoparticles were determined.

Keywords: Nanoparticles; Electromagnetic levitation; Gas condensation; Ti; TiO_2

1. Introduction

Titanium nanoparticles have been used as doping agents to improve the hydrogen storage and exchange properties of sodium alanate, which may find important applications in mobile devices. Additionally, titanium nanoparticles formed at the metal-tissue interface may play an important role in the long term stability of titanium-based biomedical implants [1]. Titanium dioxide is used largely in technological applications. It is currently being used as a white pigment for paints or cosmetics, as a support in catalysis and as a photocatalyst. Titanium dioxide is also a common material for photovoltaic cells and appears to be interesting as a dielectric material for the next generation of ultra-thin capacitors due to its high dielectric constant [2].

Electromagnetic levitational gas condensation is a one-step process for the synthesis of metallic nanoparticles. The first successful experimental work for the electromagnetic levitation melting was performed by Okress et al. [3]. Among all the other production methods of nanoparticles, this method can lead to a much higher production rate and a lower level of contamination. Bigot and Champion reported the first attempts on using the electromagnetic levitation melting for synthesis of nanoparticles iron, nickel, cobalt, chromium, copper and aluminum [4]. Also, Rhee et al. have synthesized metallic, metallic oxide and intermetallic nanoparticles using levitational gas condensation method [5]. Recently, Kermanpur et al. have synthesized metallic NPs of Al, Fe, Zn and ZnO by the ELGC method [6-8].

In the present project, a novel electromagnetic levitational gas condensation (ELGC) system was simulated, designed and manufactured for the synthesis of titanium and titanium dioxide nanoparticles. Pure titanium as the charge metal, argon gas as the condensation medium and oxygen gas as the reacted gas for producing the oxide of nanoparticles were used in the ELGC method. The best process parameters for the synthesis of titanium and

Department of Materials Engineering, Isfahan University of Technology Isfahan 84156-83111, Iran

Corresponding author:
M. Moazeni, Department of Materials Engineering, Isfahan University of Technology Isfahan 84156-83111, Iran
Email: maryam_moazeni@mmaterialeng.com

titanium dioxide nanoparticles were determined.

2. Materials and Experiments

2.1. Simulation of induction coil

A suitable induction coil for the electromagnetic levitation melting of titanium was designed by finite element simulation of electromagnetic force using commercial software ANSYS. Geometry of the coil used for levitation and evaporation of titanium has been shown in figure 1. The suitable design for levitating Ti sample included a cylinder with four turns at the lifting part along with five turns wound at the opposite direction at the stabilizing part. The distance between the lifting and stabilizing parts was about 10 mm.

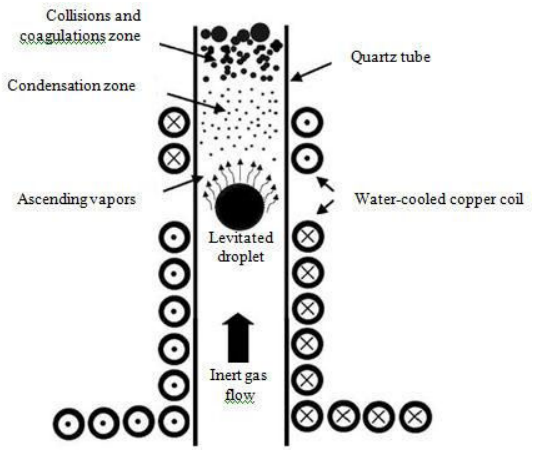

Fig. 1. The model geometry for electromagnetic levitation melting of titanium.

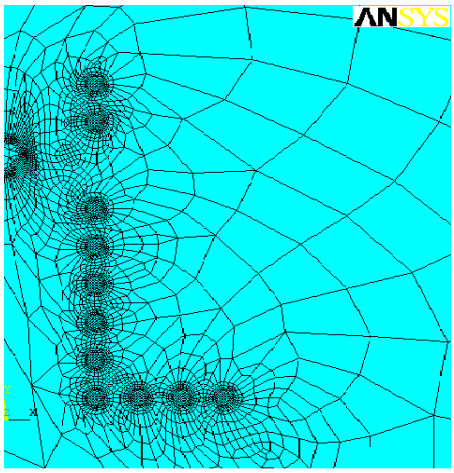

Fig. 2. The entire finite element mesh used for the coupled-field analysis.

Figure 2 shows the finite element mesh used in the electromagnetic calculations comprising air, coil, sample and the water-cooled space inside the coil. Gravitational force was introduced to every single node of the sample domain. This was due to the nature of this kind of force which is exerted on bulk of the sample and not only the surface.

2.2. Experimental procedure for synthesis of Ti and TiO_2

Experimental set-up of the ELGC rig is shown schematically in Figure 3. The particle production unit is made of a quartz tube (3) located inside a special shaped induction coil (2) for levitation. The coil is connected to a radio-frequency generator power supply (1) working under 450 kHz and 45 kW. The particle collection unit is equipped with a bubble containing ethanol.

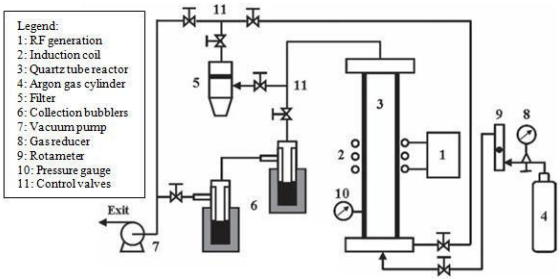

Fig. 3. Schematic of the experimental set-up of the ELGC system.

In the experimental procedures for synthesis of titanium, the argon gas was fed into the reactor with a given flow rate. An alumina crucible containing about 5 gram of a titanium sample with the purity of 99.9 wt% was positioned within the appropriate coil using the withdrawal mechanism of the system (not shown in the figure). Prior to running the apparatus, the pressure and gas flow rate of the reactor were set according to the predefined values. The crucible was rapidly pulled down out of the coil when the power supply was turned on. In this state, the sample was levitated and then was started to heat up, melt and vaporize. The titanium vapors which have been surrounding the molten droplet, were condensed by the argon gas stream flowing

upward in the reactor. The condensed particles were finally collected in ethanol.

The experimental conditions for production of Ti are listed in Table 1. Temperature of the levitated droplet was measured using a Minolta/Land Cyclops 152 infrared pyrometer. Calibration of the pyrometer was based on adjusting the accurate value of the emissivity coefficient of the measurement medium.

The titanium dioxide nanoparticles were synthesized by injection of oxygen gas in different flow rates and argon with flow rate of 15 lit/min into the reactor. Table 2 shows the flow rates of reacted gas and temperature of Ti droplet.

Table 1. The experimental conditions for synthesis of Ti.

Experiment Number	Argon flow rate [lit/min]	Temperature of Ti droplet [K]
1	5	2223
2	15	2173
3	25	2123

Table2. The experimental conditions for synthesis of TiO_2.

Experiment Number	Oxygen flow rate [lit/hr]
1	10
2	20
3	30

The morphology and structure of the synthesized nanoparticles were characterized by scanning electron microscopy (SEM Philips X230) and XRD (Bruker, D8ADVANCE with Cu Kα anode) and size of particles were measured by image tools.

3. Results and discussion

3.1. Results of simulation

The outputs of simulation, basically read from post-processing menu in the software, included nodal temperature, Joule heating, thermal flux and gradient, electric field, Lorentz force and 2-D flux lines. The simulated electromagnetic flux distribution in the model is shown in figure 4, confirming the equilibrium position for the Ti sample for this coil.

The simulated distribution of temperature within the Ti sample after about 20 seconds was shown in figure 5. The measured temperature of the sample surface was about 2200K after 20. Although the results of

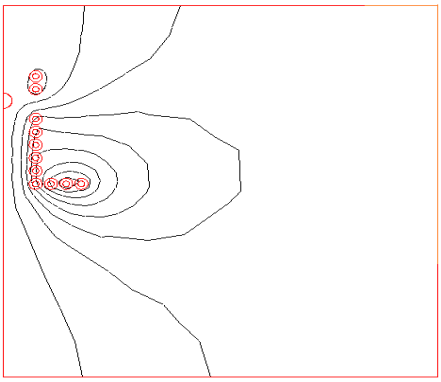

Fig. 4. Distribution of the electromagnetic flux in the coil having the coil angle of zero, showing the equilibrium position for the Ti sample.

simulation show that the maximum temperature of sample is about 4590 K, this temperature in only a few nodes and most of the nodes have temperatures between 1600 – 3000 K. Also, the difference between the experimental and the simulation data was due to both the model approximations and the errors of the temperature measurements; the inner wall of the quartz tube was quickly covered by the Ti vapors and this caused error in the infrared pyrometer readings. The simulation results clearly show the skin effect of the radio frequency induction field on the sample surface.

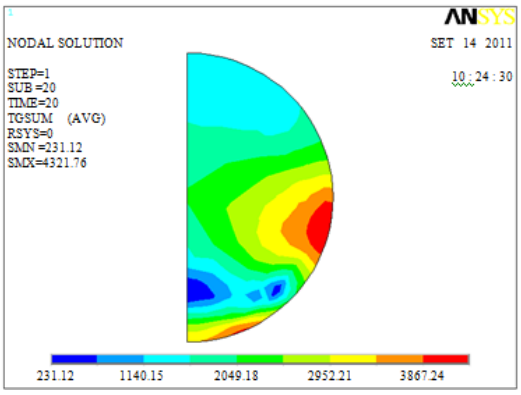

Fig. 5. Temperature distribution (in K) within the Ti sample during levitation after 20 seconds.

The sample temperature in surface was sufficient to vaporize the sample for the subsequent formation of Ti nanoparticles.

3.2. Characterization of the titanium nanoparticles

The SEM micrographs of the titanium particles synthesized by the ELGC method using argon flow rate of 5, 10 and 15 lit/min under atmospheric pressure are shown in Figures 6. The particles are spherical having a size of 96 ± 24, 76 ± 26 and 116 ± 34 nm, respectively. Note that the particles shown in the micrographs are oversized by 40 nm due to the gold layer coated on the particles. It is clearly observed that in atmospheric pressure, with increasing of argon flow rate from 5 to 15 lit/min, the particle size decreased, then in flow rate of 20 lit/min, the size of particles increased. This may describe that a higher argon flow rate reduces the time in which the condensed particles could grow and coalesce, however, the higher argon flow rate can also derive the turbulent flow leading to particle collisions and coalescence in the reactor and it may cause larger particle size in flow rate of 20 lit /min. Therefore, to produce spherical nanoparticles of titanium and titanium oxide with small size and narrow size distribution, flow rate of argon should be about 15 lit/min. It should also be noted that, a higher argon gas is preferable as it has a direct effect on the production rate of the process.

The XRD pattern of the titanium particles synthesized by this method showed in figure 7. This figure illustrates the XRD pattern of the Ti synthesized particles. The patterns clearly show the crystalline titanium particles.

3.3. Characterization of the titanium dioxide nanoparticles

Figure 8 a–c shows SEM micrographs of TiO_2 particles synthesized using Ar gas under flow rates of 15 and oxygen under flow rate of 10, 20 and 30 lit/hr at pressure of 760 mm Hg. The particles are almost spherical in shape with the mean size of 78.34±58, 59.11±27 and 119.08±38nm, respectively.

According to the SEM micrographs, it is seen that increasing the Ar flow rate, obtained the same results for synthesis of Ti.

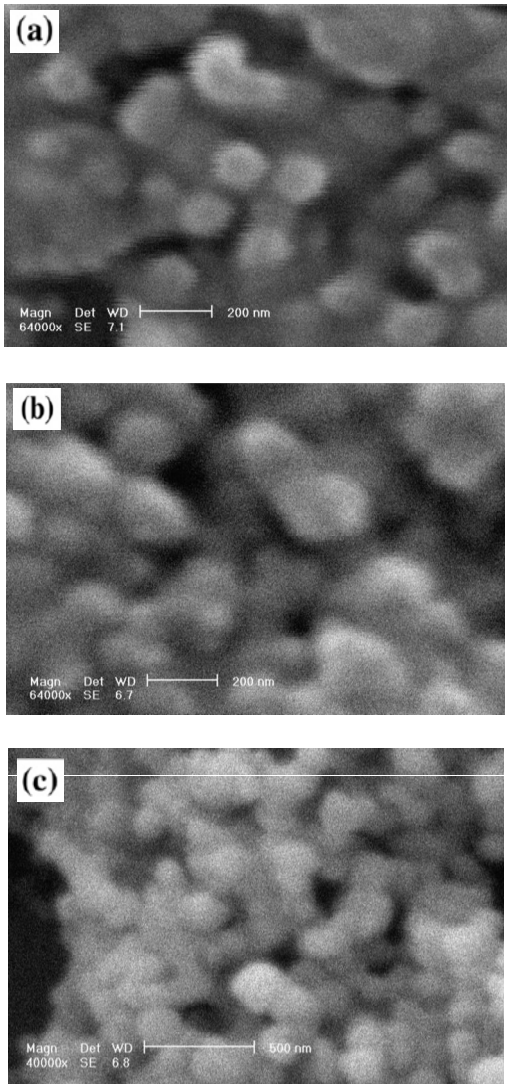

Fig. 6. SEM micrographs of the Ti particles using different argon flow rates: (a) 5 lit/min, (b) 15 lit/min, (c) 20 lit/min.

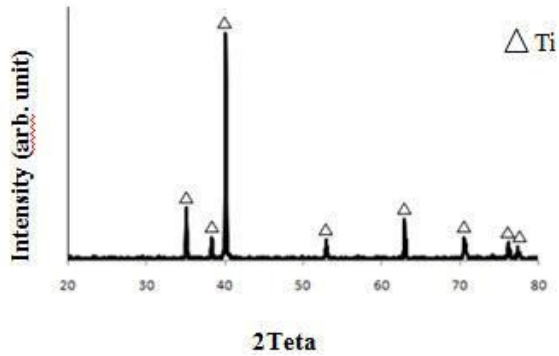

Fig. 7. XRD pattern of the titanium particles.

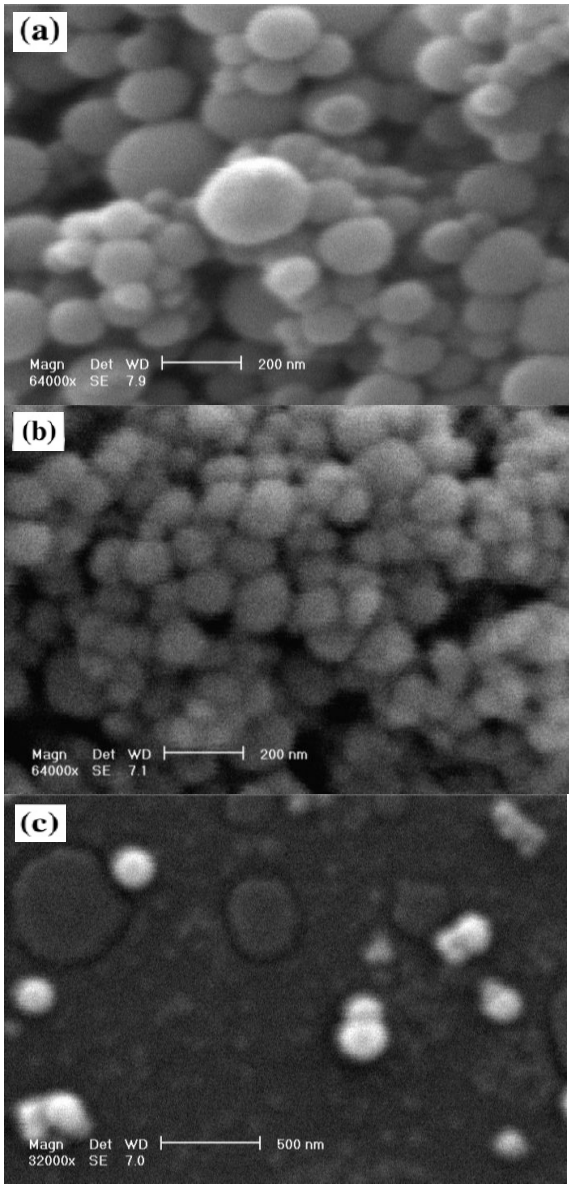

Fig. 8. SEM micrographs of the TiO_2 particles under argon with flow rate of 15 lit/min and different oxygen flow rates: (a) 10 lit/hr, (b) 20 lit/hr, (c) 30 lit/hr.

4. Conclusions

A suitable levitation coil was designed by ANSYS software for the process. This induction coil has a cylinder with four turns at the lifting part along with five turns wound at the opposite direction at the stabilizing part. The present study showed that the titanium and titanium dioxide nanoparticles can be successfully synthesized using pure titanium charge material as well as suitable argon and argon-oxygen mixture at different flow rates by the ELGC system under atmospheric pressure. The nanoparticles of Ti and TiO_2 had a spherical shape whose size depended upon the gas flow rate used in the process. Using the present ELGC system, Ti nanoparticles with the size of about 76 nm and TiO_2 nanoparticles were 57 nm, were synthesized by argon and oxygen flow rates were 15 lit/min and 10 lit/hr, respectively.

Acknowledgments

We would like to thank Eng. Karbasi for her assistance in SEM laboratory and Eng. K. Saebi for his help in designing the experimental rig.

References

1. Ghosh, D., Pradhan, S., Chen, W., Chen, S., *Chem. Mater.,*Vol. 20 (2008) pp. 1248-50.
2. Pottier, A., Chane, C., Tronc, E., Mazerollesb, L., Jolivet, J. P., *J. Mater. Chem.,* Vol. 11 (2001) pp. 1116-21.
3. Okress, E. C., Wroughton, D. M., Comentz, G., Brace, P. H., Kelly, J. C., *J. Appl. Phys.,*Vol. 23 (1952) pp. 545-52.
4. Champion, Y., Bigot, J., *NanoStruct. Mater.,* Vol. 10 (1998) pp. 1097-100.
5. Uhm, Y. R., Han, B. S., Lee, M. K., Hong, S. J., Rhee, C. K., *Mater. Sci. Eng., A,* Vol. 449-51 (2007) pp. 813-16.
6. Vaghayenagar, M., Kermanpur, A., Abbasi, M. H., Ghasemi Yazdabadi, H., *Adv. Powder Technol.,* Vol. 21 (2010) pp. 556-63.
7. Kermanpur, A., Nekooei Rizi, B., Vaghayenegar, M., H. Ghasemi Yazdabadi, *Material Letters,* Vol. 63 (2009) pp. 575-77.
8. Kermanpur, A., Dadfar, M. R., Eshraghi, M., *J. Nanosci. Nanotechno.,* Vol. 10 (2010) pp. 1–5.